Catal Lett (2009) 130:72–78
DOI 10.1007/s10562-009-9903-4

Silica-Supported Cobalt Catalysts for Fischer–Tropsch Synthesis: Effects of Calcination Temperature and Support Surface Area on Cobalt Silicate Formation

A. H. Kababji · B. Joseph · J. T. Wolan

Received: 19 December 2008 / Accepted: 10 February 2009 / Published online: 3 March 2009

Abstract Cobalt silicate formation reduces the activity of the catalyst in Fischer–Tropsch synthesis (FTS). In this article, the effects of calcination temperature and support surface area on the formation of cobalt silicate are explored. FTS catalysts were prepared by incipient wetness impregnation of cobalt nitrate precursor into various silica supports. Deionized water was used as preparation medium. The properties of catalysts were characterized at different stages using FTIR, XRD and BET techniques. FTIR-ATR analysis of the synthesized catalyst samples before and after 48 h reaction identified cobalt species formed during the impregnation/calcination stage and after the reduction/reaction stage. It was found that in the reduction/reaction stage, metal-support interaction (MSI) added to the formation of irreducible cobalt silicate phase. Co/silica catalysts with lower surface area (300 m^2/g) exhibited higher C_{5+} selectivity which can be attributed to less MSI and higher reducibility and dispersion. The prepared catalysts with different drying and calcination temperatures were also compared. Catalysts dried and calcined at lower temperatures exhibited higher activity and lower cobalt silicate formation. The catalyst sample calcined at 573 K showed the highest CO conversion and the lowest CH_4 selectivity.

Keywords Cobalt catalyst · Fischer–Tropsch synthesis · Metal-support interaction · CO hydrogenation

1 Introduction

The increased global demand for clean fuels has led to increased interest in the production of clean liquid fuels from sources other than petroleum. Fischer–Tropsch synthesis (FTS) can be used to convert coal, natural gas or biomass to clean fuels and chemicals via syngas. Cobalt based catalysts are advantageous for the conversion of natural-gas-derived synthesis gas because they are relatively inexpensive and have low water–gas shift activity [1]. Supported cobalt catalysts are also preferred for FTS when high per pass conversion, longer life-times, and higher selectivities to paraffinic products are needed. To increase activity, cobalt is usually deposited on a high surface area oxide such as alumina or silica supports to obtain high metal dispersion. FTS activity of supported cobalt catalysts depends on the number of active sites on the surface of crystalline cobalt metal which is determined by the cobalt particle size, dispersion, loading, and degree of reduction [2–4]. Structural and chemical properties of the support also influence catalytic activity and product selectivity. Support surface modifications can affect metal-support interaction (MSI), reducibility and dispersion of cobalt species to enhance the formation of desirable cobalt species. The cobalt oxide phases (CoO and Co_3O_4) are considered desirable and easily reduced to active metallic cobalt particles [5]. These oxides deposit on the silica surface when the precursor cobalt nitrate solution is decomposed. Synthesis of highly dispersed cobalt catalyst requires strong interaction between the support and the cobalt precursor, but such strong interactions, generally, lower reducibility of such precursors and promote the formation of undesired phases such as cobalt silicate [6]. Cobalt silicate is considered inactive for FTS since it has no cobalt-metal sites. Tsubaki et al. [7] found that the

---

A. H. Kababji · B. Joseph · J. T. Wolan (✉)
Department of Chemical and Biomedical Engineering,
University of South Florida, Tampa, FL 33620, USA
e-mail: wolan@eng.usf.edu

texture, crystallite phase and acidity of silica are influenced by the hydrothermal treatment with solutions. The reducibility of supported cobalt was closely associated with the silica surface properties. The concentration, distribution, and nature of hydroxyl groups (silanols) on the silica surface also play an important role in the formation of cobalt species and later the dispersion of supported metal on the silica surface [8]. Ming and Baker [9] reported that the catalytic performance of cobalt–silica gel FTS catalyst was strongly affected by preparation conditions such as the pH value of the impregnation solution which changed the interaction of cobalt and silica support, resulting in different MSI, dispersion and reducibility of the supported cobalt species.

Prior work done on Co/silica-supported catalysts has mainly focused on cobalt dispersion, reduction, preparation and pore size distribution. In this study, the cobalt species-support interaction leading to the formation of undesired cobalt silicate phase and, its influence on the activity and performance of the catalyst are presented. Once formed, it is difficult to reduce cobalt silicate to active metallic sites at FTS reaction temperatures [10]. The reported results suggest disagreement on the chemistry and stage at which cobalt silicate form. Kogelbauer et al. [11] found that the presence of cobalt metal is necessary for cobalt silicate formation and is enhanced by the presence of H_2 depending on exposure time and gas phase concentration. Other literature findings [12, 13] have postulated that an intermediate cobalt silicate surface phase is formed during the initial decomposition of the cobalt nitrate precursor during preparation or by a reaction between the aqueous cobalt complexes and surface silanol groups which is enhanced by using metal salts decomposed during thermal treatment. Ernst et al. [14] attributed the formation of cobalt silicate during reduction to the reaction of unreduced CoO with silica to form high surface area cobalt orthosilicate:

$$2CoO + SiO_2 \rightarrow Co_2SiO_4$$

Puskas et al. [10] proposed a more detailed reaction pathway:

$$CoO + H_2O \rightarrow Co(OH)_2$$
$$Co(OH)_2 + SiO(OH)_2 \rightarrow CoSiO_3 + 2H_2O$$

The reaction of finely dispersed cobalt oxide and water during reduction result in molecular cobalt hydroxide formation. Migrating silicic acid then reacts with cobalt hydroxide to produce cobalt silicate. This mechanism can also occur following impregnation in water during the preparation and drying/calcination stage. The active surface silanol groups form silicic acid which reacts with cobalt hydroxide to form highly amorphous FT-inactive cobalt silicate [11]. In this paper, the effects of the support surface area and the calcination temperature on cobalt species-support interaction are investigated. These parameters affect the chemistry and stage of formation of cobalt species such as cobalt silicate. Furthermore, the surface area of the silica support can remarkably influence the resultant FTS catalyst performance. The MSI during preparation, drying and calcination is an important aspect in the synthesis of highly active FTS catalysts.

2 Experimental

2.1 Catalyst Preparation

Commercially available silica gel (Davisil grade 646, 635 and 710) was used as a support. An aqueous solution of cobalt nitrate was impregnated into the various silica supports by incipient wetness impregnation (IWI) method using appropriate volume of deionized water. Aqueous ammonium hydroxide was added to adjust the pH. The loading of cobalt was 20 wt% for all catalyst samples. The particle size was kept between 0.25 and 0.5 mm. The series of supported Co catalysts, silica supports structural properties, drying and calcination times and temperatures are shown in Table 1.

The calcined samples were reduced in H_2 at 623 K for 12 h at high space velocity (2,000 h^{-1}) and 1 atm at a ramping rate of 1 K min^{-1}. Co/silica catalyst ID: 300Co-1 was used as a comparing reference. Catalysts 1–3 have

Table 1 Silica-support structural properties used in preparing catalyst samples and their drying and calcination conditions

Catalyst ID	Silica support properties			Drying Temperature/time (K)/h	Calcination Temperature/time (K)/h
	Pore vol (cm^3/g)	Pore Dia (nm)	BET SA (m^2/g)		
300Co-1	1.15	15	300	298/24	573/3
480Co-2	0.75	6	480	298/24	573/3
560Co-3	0.7	5	560	298/24	573/3
300Co-4	1.15	15	300	393/16	673/3
300Co-5	1.15	15	300	393/16	773/3

different silica support characteristics but were prepared under the same controlled conditions. Catalysts 1, 4 and 5 have the same silica support characteristics (Davisil-646) differing in drying and calcination conditions only.

The FTS reaction was carried out in a fixed-bed catalytic reactor consisting of a tube with an inner diameter of 6 mm placed in a programmable furnace. The reduced catalyst of 1.0 g was loaded vertically in the reactor. Void fraction was calculated to be around ~15%. Gas flows were regulated via programmable flow controllers with a static, inline mixer prior to the furnace inlet. The reaction conditions were P (total) = 0.8 MPa, $T = 503$ K, CO/H_2 = 1/2. Gas space velocity was kept at 1,500 h^{-1}. The reaction product samples were taken at 1 h intervals and analyzed by on-line FTIR and GC. The analysis of hydrocarbons dissolved in a solvent after condensing in a cold trap was carried out with GC-FID using a customized DB-2887 column. Steady state was reached after 6 h time-on-stream. The reaction time was as long as 48 h, and the activity of the catalyst was relatively stable during this time period.

2.2 Catalyst Characterization

The XRD spectra of the catalysts were measured using a Philips Pananlytical X'Pert X-ray diffractometer using Cu Kα radiation in a 0.02° step-scan mode in the 20–75°2θ angular regions. A tube power of 40 kV and 30 mA was maintained for all runs. The BET surface area and pore volume of the catalysts were determined by N_2 physisorption using a Quantachrome AUTOSORB-1 automated system. Each sample was degassed in the system at 573 K for 4 h prior to N_2 physisorption.

A BIO-RAD Excalibur FTS3000 FTIR equipped with a permanently aligned gas cell was used to analyze the effluent. The 60 mm diameter gas cell provided an infrared beam path length of 2.4 m and consisted of a borosilicate glass body with a KBr window and a total volume of 0.1 L. A linearized mercury cadmium telluride (MCT) detector was used, with an effective range of analysis between 600 and 4,000 cm^{-1} wavenumbers. To obtain spectra of the fresh, calcined and reacted (48 h) powder catalysts, a Pike-Technologies diamond MIRacle single reflection horizontal attenuated total reflectance (HATR) unit designed for use in the FTIR spectrometer was utilized. 500 scans were recorded for each sample at a resolution of 4 cm^{-1}.

3 Results and Discussion

3.1 Cobalt Oxide Phase Verification

X-ray diffraction was used to verify the co-existence of cobalt oxide species following impregnation/calcination and after 48 h reaction time. The XRD patterns of selected catalysts at different stages are illustrated in Fig. 1.

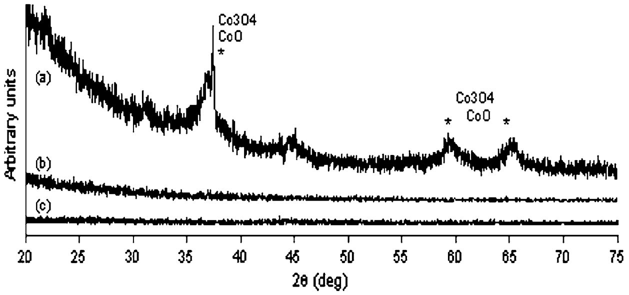

Fig. 1 The XRD patterns of catalysts: **a** Calcined 560Co-3, **b** after 48 h FTS 560Co-3 and **c** after 48 h FTS 300Co-5

Sample 560Co-3 after calcination but before reaction showed diffraction peaks at 36.8°, 45.1°, 59.5° and 65.5° indicating the presence of CoO and Co_3O_4. XRD measurements of the remaining catalysts after calcination showed similar patterns but with different peak intensities. The two oxides can co-exist on the catalyst surface after calcination. Large clusters of Co_3O_4 can form via oxidative aggregation of small amounts of CoO [5, 10]. Following reduction and 48 h FTS, the XRD diffraction peaks of sample 560Co-3 have disappeared, indicating structural irregularity and no cobalt oxide. However, highly amorphous cobalt silicate could exist on the surface after FTS reaction. The used catalyst 300Co-5 XRD patterns also showed no cobalt oxide species on the catalyst surface. Therefore, XRD is not preferred for amorphous cobalt silicate identification. Further characterization using IR spectroscopy was required to verify the effects of surface area and calcination temperature.

3.2 FTIR-ATR Analysis

Selected IR spectra are shown in Fig. 2. All catalyst samples were analyzed using IR spectroscopy to investigate the effect of varying the surface area on the MSI which could lead to the formation of cobalt silicate. Figure 2a shows the absorption of silica (1,100, 975, 800 cm^{-1}) for the dried catalyst 300Co-1. The spectrum also confirms the absorbance of the nitrate group (1,610, 1,365, 842 cm^{-1}) [15] indicating the existence of some cobalt nitrate residue due to low drying temperature. The spinel Co–O bond absorbance peak corresponding to Co_3O_4 is clearly visible around 667 cm^{-1}. Another weak Co–O absorbance peak exists around 580 cm^{-1} probably due to small amounts of CoO formation. The small amounts of CoO are explained by the possible oxidative aggregation of CoO to large clusters of Co_3O_3. Figure 2b represents the dried catalyst sample 480Co-2 which has similar IR features as sample 300Co-1 as well as the other dried catalyst samples

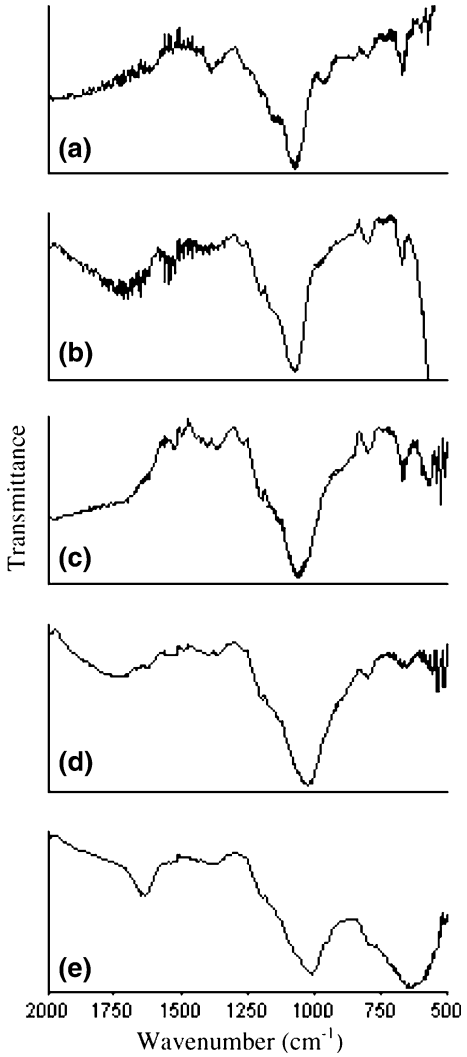

Fig. 2 Selected IR spectra of catalyst samples: **a** Dried 300Co-1, **b** dried 480Co-2, **c** Calcined 300Co-1, **d** calcined 560Co-3 and **e** after 48 h FTS 480Co-2

prepared but with different peak intensities. It is also observed that the ratio of the intensity of the Co–O peak assigned to Co_3O_4 to the Si–O silica stretching peak intensity in spectrum (b) is less than the ratio of the Co_3O_4 peak to the silica peak in spectrum (a) sample 300Co-1. Furthermore, the dried sample 480Co-2 spectrum does not show any indication of CoO formation. This leads to the conclusion that lower surface area sample 300Co-1 contained more desired surface cobalt oxide species than sample 480Co-2. To explain why some catalyst samples contain more desired cobalt oxide species, we go back to the initial mixing of the cobalt precursor and the various surface area silica supports. After mixing, the cobalt positive ions are attracted to the silica support pores by adjusting the pH using aqueous ammonia so as to maintain a negative charge through the silica surface. If the pH value is 2–5 (preferably around 4.5) then the surface is negatively charged and the cobalt ions are dragged to the pores by capillary action. If the pH value is less than 2 then the silica surface is positively charged, thus repulsing the bulk of cobalt cations from the porous silica surface. Cobalt cations at pH less than 2 and higher than 5 can react with hydrated silica surface (SiOH groups) forming cobalt silicate. In addition, these cations can react with the nitrate ions and the surface SiOH groups forming complexes that could hinder the deposition of cobalt ions in the pores thus affecting the dispersion of cobalt ions and ultimately upon drying and calcination the amount of desired cobalt oxide species formed. Lower support surface area leads to less surface SiOH group formation during preparation and thus less MSI. Puskas et al. [15] found using infrared spectroscopy much less than expected Co_3O_4 formation upon calcination when silica was used as a support. This is also explained by the reaction between CoO and SiO_2 during calcination which prevented large amounts of CoO from further oxidation to form Co_3O_4. Interestingly, sample 480Co-2 does not show any nitrate ion peak absorbencies. This is due to a possible interaction between the hydrated silica in the higher surface area sample 480Co-2 and the nitrate ion during preparation. The peak around 1,640 cm^{-1} is assigned to hydroxyl groups. The dried sample 480Co-2 contains more hydroxyl groups (SiOH) than the dried sample 300Co-1. Thus, the existence of silanol groups (SiOH) on the silica surface plays an important role in the formation of cobalt species.

The calcined spectrum of sample 300Co-1 (Fig. 2c) is shown. Si–O stretching bands are clearly visible. As expected, the absorption peaks of Co_3O_4 are confirmed around 667 and 580 cm^{-1}. The calcined spectra of other samples were essentially the same but with different peak intensities. The spectrum (d) of calcined sample 560Co-3 in Fig. 2 confirmed the effect of surface area on the resultant cobalt species formed on the support surface. While Co_3O_4 is confirmed on the surface by the Co–O vibration band at 667 cm^{-1}, it is also noticed that the broad absorbance peak of Si–O (1,100 cm^{-1}) has disappeared and a new broad peak around (1,020–1,036 cm^{-1}) assigned to Si–O-Co bond has formed. This is the characteristic peak assigned to cobalt silicate [16]. The high support surface area of sample 560Co-3 has enhanced the interaction of silica and the cobalt cations during the initial decomposition of the cobalt nitrate precursor upon mixing in the presence of water. This resulted in the formation of aqueous cobalt complexes as well as the attraction of less cobalt ions to the pores. Upon drying and calcination, less cobalt oxide species was formed as evident when comparing the ratio of silica to cobalt oxide absorbance peaks in both spectra (c) and (d). Cobalt silicate formation is enhanced by using metal salts decomposing during thermal treatment

[13, 17] and is a result of a reaction between the aqueous cobalt complexes and silanol groups existing on the silica surface. The calcined sample 300Co-5 (not shown) had a similar spectrum as spectrum (d) but with less cobalt silicate peak intensity which indicates that high drying and calcination temperatures also facilitate cobalt silicate formation due to sintering and silica migration as well [13, 15, 16]. Surface area supports higher than 560 m^2/g resulted in strong interaction between the silica surface and the cobalt cations during preparation leading to the formation of more cobalt complexes and undesired cobalt silicate. Indeed, Puskas et al. [15] found that the rate of cobalt silicate formation correlates to the surface area of the silica support.

The last spectrum (e) of sample 480Co-2 after 48 h FTS confirms the formation of cobalt silicate during the reduction and reaction stage via the unreduced CoO reaction with silica mechanism in the presence of water [14]. Water is formed during H_2 reduction and as a byproduct during FTS. Furthermore, Puskas et al. [15] inferred that the high cobalt loading (13–30 wt%) generated more water during reduction resulting in formation of large amounts of cobalt silicate. Our FTIR results agree with their findings, since the loading percentage of cobalt in our samples was kept at 20 wt% and that considerable amounts of cobalt silicate were formed upon reduction as a result of the large amount of water generated. This also supports the conclusion that cobalt silicate formation is a water-induced mechanism.

Any cobalt species not reducible during the H_2 reduction stage up to 1,073 K has been identified as cobalt silicate [18]. However, the amount of cobalt silicate formed during reduction differs. An important feature in spectrum (e) is that the intensity of cobalt silicate assigned peak and cobalt oxide assigned peak is almost the same for sample 480Co-2. This result was also true for sample 300Co-1 after 48 h reaction time. The amount of cobalt oxide in those two samples after reaction is still considerable meaning those two samples can still carry on FTS for longer periods of time. The ratio of the assigned cobalt oxide peak to the assigned cobalt silicate peak in those two samples is much higher than the same ratio for sample 560Co-3 as shown in spectra (e) and (d), respectively.

3.3 Effect of Drying and Calcination Temperature

BET was used to study the loss of surface area (SA) for all catalyst samples after calcination and reaction as shown in Table 2. All catalysts were degassed for at least 4 h at 573 K before N_2 physisorption to ensure all products formed in the pores were eluted. It was found that the loss of surface area after calcination depends on the calcination temperature, the higher the calcination temperature the more significant the surface area loss as is evident in sample 300Co-5. This is due to silica migration which occurs at temperatures higher than 573 K for silica [10, 13, 19]. It is known that high surface area (>200 m^2/g) reactive silica favors silica migration [15]. Furthermore, the loss of SA can also be attributed to the filling of pores with impregnated cobalt species.

The loss in surface area after reaction is attributed to cobalt particle agglomeration which occurs during H_2 reduction where cobalt metal atoms agglomerate forming larger crystalline metal particles. Another reason for this loss is that the long chain HC products which form during the reaction but fail to desorb from the surface result in clogging of the surface pores which leads to further loss in surface area. This explains the drop in the BJH adsorption pore volume for catalyst samples after reaction. It's also noticed that the difference in surface area loss is more evident after calcination than after reaction, this is attributed to the formation of high SA amorphous cobalt silicate as a result of MSI during reduction which counters the loss in surface area due to cobalt particle agglomeration or silica migration. From the IR and BET results on all sample catalysts after calcination and after 48 h reaction, it was found that the activity to FTS was in the following order: sample 300Co-1 > 480Co-2 > 300Co-4 > 560Co-3 > 300Co-5.

3.4 Catalyst Performance and Activity

Fischer–Tropsch synthesis reaction was conducted for 48 h in a fixed-bed micro reactor for all catalyst samples. Performance parameters after reaching steady state (6 h) are reported in Table 3. It can be seen from Table 3 that sample 300Co-1 exhibited the highest CO conversion (78.1) and the lowest CH_4 and CO_2 selectivity. The space time yield (STY) and activities are also the highest for this sample and drop as the surface area of the catalyst increases. As discussed earlier, large surface area of the support increases MSI resulting in formation of cobalt silicate which in turn, limits the number of active metallic sites. The pore size of the silica support affects the rate of CH_4 production as is evident by samples 480Co-2 and 560Co-3 (6 and 5 nm, respectively). Small pore diameter is expected to promote the formation of CH_4 where a large pore diameter >10 nm increases the probability of longer HC chain formations as is evident in sample 300Co-1. The low reaction pressure (8 bar) decreases the solubility of CO and H_2 thus increasing the reaction rate to form larger amounts of CO_2. Furthermore, the relatively low reaction temperatures (~503 K) and partial pressure of CO and water enhance the water–gas shift to CO_2 and H_2 production, thus resulting in higher selectivity to CO_2. The drying and calcination temperatures had a higher impact on the

Table 2 BET surface area and BJH adsorption pore volume for all catalyst samples used in the FTS

Catalyst ID	BJH pore volume (cm^3/g)			BET surface area[a] (m^2/g)		
	Support	Calcined	After 48 h. reaction	Support	Calcined	After 48 h reaction
300Co-1	1.15	0.85	0.73	300	254	231
480Co-2	0.75	0.67	0.57	480	356	319
560Co-3	0.70	0.59	0.50	560	408	375
300Co-4	1.15	0.82	0.66	300	243	206
300Co-5	1.15	0.68	0.48	300	209	168

[a] Error of measurement = ±10%

Table 3 Catalytic performance of cobalt silica-supported catalysts in FT synthesis

Catalyst ID	STY[a] (g HC L^{-1} h^{-1})	Activity[b] (h^{-1})	CO conv. (%)	Selectivity (%)			
				CH_4	CO_2	$C_{2\text{–}4}$	C5+
300Co-1	137	0.29	78.1	4.7	8.6	7.2	79.5
480Co-2	125	0.26	70.7	10.4	9.3	8.9	71.4
560Co-3	98	0.20	62.4	9.5	14.8	13.6	62.1
300Co-4	86	0.18	59.3	8.4	14.7	9.9	67.0
300Co-5	74	0.15	55.6	8.3	21.0	11.0	59.7

Reaction conditions: 0.8 MPa, 503 K, CO/H_2 = ½, gas space velocity 1,500 h^{-1}

Weight of catalyst = 1.0 g, Co loading = 20 wt%

[a] Space time yield (STY): Grams hydrocarbon product per catalyst bed volume including voids in liters per hour operation

[b] Activity: Grams hydrocarbon product/gram catalyst used per one h operation

catalytic activity of samples 300Co-4 and 300Co-5 where the CO conversion dropped to below 60% for these two samples in comparison to sample 300Co-1 (78.1%) which has the same surface area (300 m^2/g). The higher temperatures of calcination most likely resulted in the sintering and agglomeration of the cobalt particles thus lowering the cobalt active surface area leading to lower catalytic activity after reduction. The structural properties of the silica supports (surface area and pore diameter) had a lower impact on the activity and yield than the drying and calcination temperatures. (Samples 300Co-1, 480Co-2 and 560Co-3 had higher CO conversion, activity and yield than samples 300Co-4 and 300Co-5 where the higher drying and calcination temperatures adversely impacted the catalytic activity).

The activity of Co/silica catalysts was studied with reaction time. Fig. 3 shows CO conversion as a function of time for samples 300Co-1, 560Co-3 and 300Co-5. All other samples showed similar behavior but with different CO conversion values. The CO conversion increases initially as the catalyst reaches steady state due to higher amounts of CH_4 formation. The conversion drops after 22 h, but remains relatively stable for the rest of the run. The drop in CO conversion could be a result of cobalt silicate formation which has no catalytic FTS activity. Another reason could be the filing of the support pores with HC products which can block the active cobalt sites preventing further CO hydrogenation. Sample 560Co-3 (*) showed significant drop in initial CO conversion in comparison to sample 300Co-1 due to stronger MSI which resulted in cobalt silicate formation. Sample 300Co-5 also exhibited significant CO conversion drop. This can be attributed to sintering effects occurring during the high calcination temperature process.

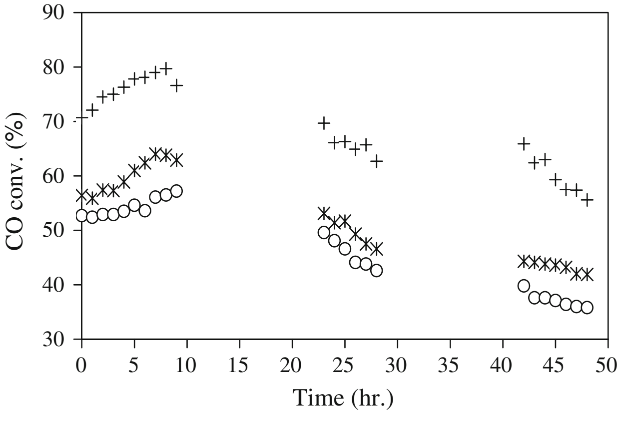

Fig. 3 CO conversion with time for samples 300Co-1 (+), 560Co-3 (*) and 300 Co-5 (O). FTS reaction time: 48 h

4 Conclusions

The results of this study indicate that the support surface area affects the MSI leading to the formation of cobalt silicate. Our results also agreed with the literature conclusion that the bulk of cobalt silicate forms during reduction as a water-induced mechanism. It was also concluded that cobalt silicate may form during the catalyst synthesis process depending on many factors such as the pH, cobalt loading percentage and surface area of the silica support and its interaction with the cobalt precursor. The activity and STY of the catalyst samples studied decreased as the surface area of the catalyst increased ($300 > 480 > 560$ m^2/g). This was also true for the CO conversion which dropped as support surface area increased. When catalysts with the same silica support surface area were used, the CO conversion decreased as drying and calcination temperatures increased from 573 to 773 K. The same trend was noticed for activity and STY. This was explained by cobalt particle agglomeration due to sintering and silica migration. The results also indicate that the properties of silica supports affect the product distribution. Catalyst with small pore diameter (<6 nm) increased the rate of CH_4 formation.

Acknowledgments Financial support from the National Aeronautics and Space Administration (NASA) grant (16266038-27) through a subcontract from the University of Central Florida is gratefully acknowledged. The authors would also like to thank Haito li and the nanomaterials and nanomanufacturing research center (NNRC) for help with the BET and XRD experiments.

References

1. Iglesia E (1997) Appl Catal A 161:59
2. Iglesia E, Soled SL, Fiato RA (1992) J Catal 137:212
3. Johnson BG, Bartholomew CH, Goodman DW (1991) J Catal 128:231
4. Fan L, Yokota K, Fujimoto K (1992) AIChE J 38:1639
5. Zhang J, Chen J, Ren J, Sun Y (2003) Appl Catal A 243:121
6. Soled SL, Baumgartner JE, Reyes SC, Iglesia E (1995) Proc Mater Res Soc Symp 368:113
7. Zhang Y, Liu Y, Yang G, Sun S, Tsubaki N (2007) Appl Catal A 321:79
8. Iler RK (1979) The Chemistry of Silica. Wiley, New York
9. Ming H, Baker BG (1995) Appl Catal A 123:23
10. Puskas I, Fleisch TH, Full PR, Kaduk JA, Marshall CL, Meyers BL (2006) Appl Catal A 311:146
11. Kogelbauer A, Weber JC, Goodwin JG (1995) Catal Lett 34:259
12. Coulter KE, Sault AG (1995) J Catal 154:56
13. Van Steen E, Sewell GS, Makhote RA, Micklethwaite C, Manstein H, de Lange M, O'Connor CT (1996) J Catal 162:220
14. Ernst B, Libs S, Chaumette P, Kiennemann A (1999) Appl Catal A 186:145
15. Puskas I, Fleisch TH, Kaduk JA, Marshall CL, Meyers BL (2007) Appl Catal A 316:197
16. Puskas I, Fleisch TH, Hall JB, Meyers BL, Roginski RT (1992) J Catal 134:615
17. Zhang Y, Wei D, Hammache S, Goodwin JG Jr (1999) J Catal 188:281
18. Jablonski JM, Wolcyrz M, Krajczyk L (1998) J Catal 173:530
19. Hilmen AM, Schanke D, Holmen A (1996) Catal Lett 38:143